IJPSR (2020), Volume 11, Issue 11 **(Research Article)**

INTERNATIONAL JOURNAL OF PHARMACEUTICAL SCIENCES AND RESEARCH

Received on 19 July 2020; received in revised form, 04 October 2020; accepted, 18 October 2020; published 01 November 2020

THE POTENTIAL ROLE OF NANOTECHNOLOGY TO CONTROL OF INDUSTRIAL BIOFILM

Chandrakant Patel * and Neelam Tripathi

Department of Microbiology, Sri Satya Sai University of Technology and Medical Science (SSSUTMS), Sehore - 466001, Madhya Pradesh, India.

Keywords:

Biofilm, Nanotechnology, Micro method, Microbiology, Microorganism, Nanoparticles.

Correspondence to Author:
Chandrakant Patel

Department of Microbiology, Sri Satya Sai University of Technology and Medical Science (SSSUTMS), Sehore - 466001, Madhya Pradesh, India.

E-mail: ckpateljaunpur@gmail.com

ABSTRACT: In recent years, most researchers and interesting ones in the field of microbial biofilm documented that nanoparticles like silver, metal ions play a significant role in the biofilm approach. Here i would like to draw your attention to the modern technique in biofilm and the role of nanotechnology in combating medical resistant microbial infection. It is now realized that most bacterially derived sessile communities are capable of forming irreversible biofilms on surfaces and interfaces by embedding themselves deep in a self-generated polymeric matrix. Most of the fungal species that form biofilms do so in a similar manner; Candida and Aspergillus are fungal species of particular interest. The mechanism of biofilm formation depends on environmental stimuli and a series of genetic and phenotypic changes in planktonic cells. To date, five different stages have been suggested during biofilm development, namely, (i) reversible-irreversible adherence, (ii) microcolony formation, (iii) 3D biofilm formation, (iv) maturation, and (v) dissemination. It is believed nanotechnology-based approaches will provide promising advancements to prevent drug-resistant biofilm infections of medical devices and biomaterials. A small number of studies have reported the use of nanoparticle (NP) coated surfaces as biofilm inhibiting agents. At the nanometer scale, materials exhibit unique physicochemical and biological properties and sometimes phenomena, such as quantum effects, not exhibited by their bulk counterparts. Nanomaterial's had a much greater surface area to volume ratios, which enhances chemical reactivities and bioactivities. Their sizes are of the same order as biomolecules that facilitate the loading of drugs and targeting entities.

INTRODUCTION: Biofilms are organized colonies of bacteria, fungi, or yeasts that form hetero-geneous entities on biotic or abiotic surfaces by secreting extracellular polymeric substances (EPS). These substances protect individual cells from hostile factors, such as immunologic defense systems, nutrient limitations, and antibacterial agents. The genotypic and phenotypic characteristics of cells in biofilms differ from those of their free-floating counterparts, and these differences make them strongly resistant to antibiotics. This resistance has been attributed to the failure of antibiotics to penetrate biofilms, the induction of multidrug efflux pumps of biofilm-specific phenotypes, and the presence of persisters.

QUICK RESPONSE CODE

DOI: 10.13040/IJPSR.0975-8232.11(11).5831-43

This article can be accessed online on www.ijpsr.com

DOI link: http://dx.doi.org/10.13040/IJPSR.0975-8232.11(11).5831-43

Basically, microbes have the ability to adhere to surfaces, including those of inert materials, synthetic polymers, and indwelling medical devices, and this leads to colonization and mature biofilm development. Furthermore, cell detachment from mature biofilms leads to infection dissemination and transmission. In fact, clinical infections caused by biofilms are a more challenging healthcare issue than those caused by planktonic cells, and microbial infections caused by bacterial biofilms on biomedical surfaces are a leading cause of death worldwide. As a result, there is an urgent clinical need to develop long-lasting biomedical materials or devices with antibacterial and anti-biofilm surfaces [1-10].

It is believed nanotechnology-based approaches will provide promising advancements to prevent drug-resistant biofilm infections of medical devices and biomaterials. A small number of studies have reported the use of nanoparticle (NP) coated surfaces as biofilm inhibiting agents. Nanomaterials have the much greater surface area to volume ratios, which enhances chemical reactivities and bioactivities, and their sizes are of the same order as biomolecules. Furthermore, NPs are small enough to penetrate microbial cell walls and even biofilm layers that can cause irreversible damage to cell membranes and DNA. In addition, they have long plasma half-lives, and their high surface to volume ratios facilitate the loading of drugs and targeting entities [11].

MATERIALS AND METHODS:

(i) Bacterial Strains *Escherichia coli*: K-12 MG1655 wild type (WT) and mutant strains (Δ) have been used in this study and were kindly provided by the National Institute of Genetics, Japan. The mutants were *E. coli* K-12 MG1655 rpoS mutant (ΔrpoS) and *E. coli* K-12 MG1655 bolA mutant (ΔbolA).

(ii) Microbiological Media: Microbiological media and reagents were prepared using deionized water and sterilized by autoclaving at 121 °C, 15 psi for 15 min. Agar medium was subsequently cooled to 55 °C, prior to the addition of any supplements and poured into sterile plastic petridishes (BibbySterillin Ltd.) in approx. 30 ml volumes. All chemicals were purchased from Sigma-Aldrich Company Ltd. (UK).

(iii) Inoculum Preparation: A bacterial suspension was prepared by gently removing bacteria from the solid media using a sterile nichrome loop to inoculate the bacteria into a 500 ml flask containing 200 ml of sterile nutrient medium. This bacterial suspension was incubated at 37 ºC with agitation at 120 rpm for 18 h, in order to have bacteria in the exponential phase of growth.

(iv) Biofilm Plate and Assay Formation: (Crystal Violet Staining) Biofilm cells (adhered cells on the surface) used in this study were cultured and cultivated using 6 well PVC microtiter plate (Orange Scientific). 3 ml of LB media was inoculated with 300 µl of an overnight culture at OD600 was inoculated. After the incubation period (cultures reaching their mid-exponential phase) the liquid media with free-floating cells was discarded, and the wells were washed three times with distilled water to remove any planktonic cells.

Surface and wall of wells were then immediately scraped using a scraper (Orange Scientific) into 3 ml of distilled water to remove the adhered cells from the surface and then transferred to a stress assay. A biofilm formation assay was performed using a microtiter plate. 20 µl aliquots of an overnight culture with OD600 of 1.0 were inoculated into 200 µl medium in a PVC microtiter plate. After 72 h incubation, the medium was removed from wells which were then washed five times with sterile distilled water, and unattached cells were removed. Plates were air-dried for 45 min, and each well with attached cells was stained with 1% crystal violet (CV) solution in water for 45 min. After staining, plates were washed with sterile distilled water five times. At this point, biofilms were visible as purple rings formed on the side of each well. The quantitative analysis of biofilm production was performed by adding 200 µl of 95% ethanol to destain the wells. 100 µl from each well was transferred to a new microtiter plate, and the level (OD) of the crystal violet present in the destaining solution was measured at 595 nm.

Control of Biofilm: Poly (anhydride-ester) synthesis and formation of polymer-coated glass coverslips Poly [1, 6-bis (o-carboxyphenoxy)-hexanoate] were prepared [12]. Preparation of salicylic acid polymer-coated glass coverslips for microbiological assay Coated and uncoated glass

coverslips was sterilized under the Fotodyne, Inc. ultraviolet (UV) light for 2 min. Coverslips were subsequently transferred into sterile 24 well plates using sterile forceps. Culture Preparation Salmonella serovar Typhimurium MAE52 (Scher *et al.* 2005) was streaked onto Brain Heart Infusion (BHI) agar and incubated at 37 °C for 24 h. The following day a single colony was transferred into 4.5 mL of BHI broth (BD) and incubated at 37 °C overnight. The OD600 of the overnight culture was recorded using a BioRad Smart Spec 3000 spectrophotometer prior to inoculation. Sterile Falcon 24-well plates were used to grow biofilms.

Two hundred µL of *S. typhimurium* MAE52 overnight culture diluted to 10^5 CFU ml^{-1} and 1.8 mL of BHI broth with an initial pH of 7.2-7.3 was added to the experimental wells. For controls, 2 ml of BHI broth were used in the designated wells. The inoculated 24-well plates were incubated at 37 °C with gentle agitation.

Plate Count: Each experiment was performed twice in triplicate, with 500 µL samples collected at predetermined hourly time points (0, 5, 8, 12, 24, and 48 h). To break biofilms for the cell enumeration, the biofilms were placed into 4.5 ml of saline containing approximately $^{15\text{-}20}$ sterile 3 mm glass beads and vortexed for 2 minutes. Subsequently, the samples were serially diluted in BHI broth to obtain a countable range, and 100 µL were plated in triplicate.

Sample Preparation for pH and Salicylate Measurement: At each time point, the supernatants were collected, and the cells were removed by centrifugation at 1500 g (25 °C). Then, 0.45 µm syringe filters were used to sterilize the supernatant. Salicylate concentrations and pH measurements were subsequently determined.

Quantification of Salicylate Concentration: The Immunalysis Salicylates Direct ELISA Kit protocol was followed with a few modifications. The Salicylates ELISA kit-supplied salicylate standard was diluted using a 50% ethanol (v/v) solution to a range of 0-100 µg ml^{-1} for the standard curve measurement. The supplied salicylic acid standard was diluted ten times, while experimental samples were diluted to fit into a target absorbance range. Standards and samples were diluted using BHI broth (pH 7.2).

Potent Antibacterial Nanoparticles against Biofilm Control: Gentamycin Sulfate was purchased from Solarbio (Beijing, China). Phosphatidylcholine and Hydrogen tetrachloroaurate (III) were purchased from Aladdin (Shanghai, China). Citric acid monohydrate was purchased from Sinopharm Chemical Reagent Co., Ltd. All reagents were of analytical grade and used as received without further purifying. *Listeria monocytogenes*, *Staphylococcus aureus*, *Escherichia coli*, *Pseudomonas aeruginosa*, and *Salmonella typhimurium* were generous gifts received from Aurbindo pharmaceuticals limited Hyderabad.

Preparation of Nanoparticle loaded Gentamycin (GPA NPs): Phosphatidylcholine (0.065 g, 0.084 mmol) in CHCl3 (10 ml) was added to a glass vial, and the solvent was removed by rotary evaporation to provide a thin film. Then the film was dried at room temperature for 12 h to ensure that all the $CHCl_3$ was removed. Ultra-pure H_2O (10 ml) was added to the vial, shaken, and then sonicated at 25 °C for 30 min. To this cloudy solution, an aqueous solution of $HAuCl_4$ (0.029 g, 0.084 mmol in 10 ml of UP H_2O) was added dropwise with stirring. A freshly prepared aqueous solution of sodium citrate (0.125 g, 0.424 mmol in 5 ml of H_2O) was added while stirring vigorously. The pale yellow slurry became clear and then turned purple. The resulted PA NPs were rinsed twice with UP H_2O. The UV–vis spectra in H2O had a λ_{max} at 530 nm. The prepared PA NPs (0.1 mL) were mixed with gentamycin sulfate (0.2 mg/mL in UP H_2O, 0.9 mL) at room temperature in the dark. The resulting Gentamicin-PA NPs (GPA NPs) solution was initially centrifuged at 14000 rpm at 10 °C for 60 min and rinsed in UP H_2O.

Characterization of the Generated GPA NPs: The size and morphology of the GPA NPs was characterized by Hitachi S-4800 field emission scanning electron microscopy, operating at an accelerating voltage of 10 kV. To obtain high resolution images from the SEM analysis, all samples were deposited on a silicon wafer and allowed to dry. The SEM images were processed using the Image J software, and the size histograms were constructed from an analysis of 1000 particles. The hydrodynamic size and surface zeta potential were measured by dynamic light scattering measurements (Malvern Zetasizer

NANO-ZS90). The UV-visible absorption spectra were recorded on Thermo Evolution 300 spectrophotometer in the range of 300-800 nm. The gentamicin content was determined by the Sodium phosphotungstate precipitation method.

Gentamicin Load Capacity and Release Behaviors: The load capacity, defined as the ratio of the amount of gentamicin binding on the nano-particles to the initial amount of gentamicin introduced, was determined by mixing prepared PA NPs with 0.2 mg/mL gentamycin at different pH and the supernatant was obtained for measurement of free-form (no-load) gentamycin after centri-fugation. The kinetics of gentamicin release was studied from the prepared GPA NPs. In order to determine the effect of pH on the gentamicin release profiles of nanoparticles, 6 mM HEPES buffer (pH 7.4) and 6 mM Tris-HCl buffer (pH 4.5) were used, respectively. The 1 mL freshly prepared nanoparticles solution (which was incubated with gentamicin for 3 h) was initially centrifuged at 14 000 rpm at 10 °C for 60 min, and the precipitate was rinsed with UP water (1 mL). Then the GPA NPs were re-suspended in 1 mL buffer at 20 °C in tube. One tube was taken at regular time intervals (1, 2, 3, 4, 6, and 7 days), centrifuged, and the supernatant was obtained for gentamicin measurement.

Examination of Binding Affinity: GPA NPs (0.116 mg/mL, Au basis) were mixed and shaken (37 °C, 160 rpm) with bacterial samples prepared in TSB for 2 h. The samples were centrifuged at 3000 rpm for 10 min, and the binding affinity was examined by the naked eye. Minimum Inhibitory Concentration (MIC). The bacteria with a final concentration of 104 CFU/mL in TSB broth added with different concentrations of GPA NPs were incubated at 37 °C for 14 h. The optical density at 600 nm of the sample solution was recorded. Cytotoxicity Tests. The RAW 264.7 cell line was cultured in RPMI medium supplemented with 10% FBS, 100 μg/mL penicillin and 100 μ g/mL streptomycin at 37 °C in a humidified 5% CO_2 containing balanced-air incubator. Cell viability was estimated through MTT assay. The 200 μ L cells (~8000 cells) were incubated for 12 h in 96-well plates, then the medium was replaced with the medium containing different concentrations of GPA NP and incubated for another 6 h. Cells incubated in the medium containing no GPA NPs were used as a negative control (Blank). After treatment, the media containing the sample was changed with fresh media, and 10 μL of MTT (5 mg/mL) was added, and the incubation continued for 4 h. The medium was removed, and 100 μL of DMSO was added to each well to dissolve the formazan. The absorbance was measured at 570 nm. Moreover, cells grown on glass coverslips in a 24-well plate with the same treatment were fixed with 4% paraformaldehyde in PBS for 10 min. Images were obtained using a microscope.

Cellular uptake of GPA NPs: The qualitative localization of GPA NPs within cells was observed by microscopy, while the uptake of GPA NPs by cells was quantified by inductively coupled plasma mass spectrometry (ICP-MS). RAW264.7 macro-phages were plated on coverslips 12 h at 37 °C. Then the medium was replaced by a new medium containing GPA NPs (0.116 mg/mL) for 2 h. The medium was then removed, the coverslips were rinsed three times with PBS, fixed with 4% paraformaldehyde, and stained with Hoechst. The coverslips were imaged by Olympus BX53 upright microscope with a 100 × (1.30) plan oil immersion objective lens. For the ICP-MS measurements, 106 RAW264.7 cells were seeded in 6 well plates in 2 mL of complete culture medium. After 12 h, cells were incubated with 0.116 mg/mL of GPA NPs for 1, 2, 4, and 8 h. Then, the medium was removed, and cells were washed three times with PBS. Cells were trypsinized, counted, and harvested. Cells suspension was centrifuged at 200 × g for 5 min, the supernatant was transferred to a new tube. Cell pellets were digested with Aqua Regia (400 μL) and microwave (2 cycles at 950 W for 10 min).

Antibiofilm Activity: As described previously 32, 100 μL bacterial TSB solutions (~108 CFU) were seeded into 96-well polystyrene microtitre plates (Corning, NY, USA) at 37 °C for 24 h to allow biofilm formation. The non-adhered cells were removed with a pipette, and the plate was washed three times using 100 μL 0.9% (w/v) NaCl. Then existing biofilms were incubated at 37 °C in 90 μL TSB supplemented with 10 μL GPA NPs (0.116 mg/mL), equivalent Gen or PA NPs for 24 hours. Each treatment included 6 parallel wells. Biofilms incubated with TSB only were used as blank.

Biofilm mass was evaluated by Crystal violet staining assay. All experiments were performed 3-5 times. Error bars represent SD. For biofilm inhibition assay, 100 µL of bacteria in TSB (approximately 10^8 FU) were seeded into individual wells of microtiter plates in the presence of compounds for 24 h. Biofilm mass was evaluated as described above. For fluorescence microscopy, *S. aureus* or *P. aeruginosa* (~108 CFU) was grown on glass coverslips at 37 °C for 24 hours in 24-well plates supplemented with 1mL of TSB to allow biofilm formation. The coverslips were washed to remove unattached cells and were treated with GPA NPs, equivalent Gentamicin or PA NPs for 24 hours at 37 °C. Existing biofilms were treated and imaged as previous.

Nanoparticle-Based Compounds in Biofilm Control:

Antimicrobial Agents: Sodium hypochlorite solution (SH) and cetyltrimethylammonium bromide (CTAB) were purchased from Sigma (Portugal), 3-bromopropionic acid (BrOH) was purchased from Merck (VWR, Portugal), 3-bromopropionyl chloride (BrCl) was purchased from Alfa Aesar (VWR, Portugal). All dilutions were performed using sterile distilled water.

Microorganisms and Culture Conditions: The bacterium used in this study was Pseudomonas fluorescens ATCC 13525. Bacterial growth was obtained from overnight cultures (16 h) in culture medium (5 $g.L^{-1}$ glucose, 2.5 $g.L^{-1}$ peptone, and 1.25 $g.L^{-1}$ yeast extract in 0.025 M phosphate buffer, pH 7) and incubated at 30 ± 3 °C, and 150 rpm of agitation.

Antibacterial Susceptibility Tests: The minimum inhibitory concentration (MIC) of each agent was determined by the microdilution method according to the Clinical and Laboratory Standards Institute (CLSI) guidelines using 96 well microtiter plates. Bacteria at a density of 109 colony forming units (CFU) per ml were inoculated into a fresh culture medium. A volume of 200 µl was inserted in each well, along with the different concentrations of the chemicals (10% v/v). The bacterial growth was determined at 600 nm using a microplate reader. The MIC was determined as the lowest concentration at which microbial growth was inhibited. The cell suspension was plated in Plate Count Agar and incubated overnight at 30 ± 3 °C, after a neutralization step to quench the chemical's antimicrobial activity, by dilution, to sub-inhibitory concentrations. The minimum bactericidal concentration (MBC) was considered the lowest concentration of the antimicrobial agent, where no growth was detected on the solid medium.

Physicochemical Characterization Of Bacterial Surfaces: The physicochemical properties of P. fluorescent cell surface were assessed by the sessile drop contact angle measurement on bacteria lawns, performed as described by Busscher *et al.* [13] Contact angles were determined using an OCA 15 Plus (DATA PHYSICS) video-based optical measuring instrument, allowing image acquisition and data analysis. The measurements (≥ 15per liquid and chemical) were performed according to Simoes *et al.*, [14] after bacterium incubation (1 h) with the chemical at the MBC. The liquid surface tension components reference values were obtained from the literature. Hydrophobicity was assessed after contact angle measurement, following the van Oss method, where the degree of hydrophobicity of a given surface (s) is expressed as the free energy of interaction between two entities of that surface when immersed in water (w)−(ΔGsws $mJ.m^{-2}$). The surface is considered hydrophobic if the interaction between two entities is stronger than the interaction of each with water $\Delta Gsws<0$. Otherwise, if ΔGsws>0, the material is considered hydrophilic. ΔGsws can be calculated using the surface tension components of the interacting entities of equation-

$$\Delta G_{sws} = -2\left(\sqrt{\gamma_s^{LW}}-\sqrt{\gamma_w^{LW}}\right)^2+4\left(\sqrt{\gamma_s^{+}\gamma_w^{-}}+\sqrt{\gamma_s^{-}\gamma_w^{+}}-\sqrt{\gamma_s^{+}\gamma_s^{-}}-\sqrt{\gamma_w^{+}\gamma_w^{-}}\right) \text{(eq. 6.1)}$$

Where γLW, represents the Lifshitz-van der Waals component of the surface free energy and γ+ and γ− are the electron acceptor and donor parameters, respectively, of the Lewis acid-based component (γAB), where γAB=2√γ+γ−. The surface tension components of a solid material can be obtained by measuring the contact angles of three liquids with different polarities and known surface tension components (1): α-bromonaphtalene (apolar), formamide (polar), and water (polar). Upon obtaining the data, three equations of the type below can be solved:

$$(1+\cos\theta)\gamma_L^{Tot}=2\left(\sqrt{\gamma_S^{LW}\gamma_L^{LW}}+\sqrt{\gamma_S^{+}\gamma_L^{-}}+\sqrt{\gamma_S^{-}\gamma_L^{+}}\right) \text{(eq. 6.2)}$$

Where θ is the contact angle. The total surface energy is calculated as γTot=γLW+γAB.

Bacterial Surface Charge: The zeta potential of bacterial suspensions was determined in sterile water using a Nano Zetasizer. This determination was performed before and after 1 h bacterial exposure to the chemicals at the corresponding MBC.

Potassium (K+) Leakage: The quantification of K+ in bacterial solutions, before and after 1 h exposure to the MBC of each biocide was determined by flame emission and atomic absorption spectroscopy. Samples were filtrated (Whatman, pore size 0.2 µm) and analyzed in a GBC AAS 932 plus device using GBC Avante 1.33 software.

Outer Membrane Protein Extraction and Analysis: Outer membrane proteins (OMP) were isolated based on the method described by Winder *et al.*, [15]. Briefly, an overnight inoculum of P. fluorescens was washed with 8.5% NaCl solution, diluted to approximately 109 $CFU.ml^{-1}$ and incubated with each chemical at the MBC, for 1 h at 30 ± 3 °C and 150 rpm of agitation. All suspensions were then harvested by centrifugation (3202 g, 25 min) and ressuspended twice with Tris-HCl 25 mM, pH 7.4 with 1 mM $MgCl_2$.

Then, the suspension was sonicated for 2 min, 50% power (Bandelin generator with a Microtip MS 72 probe) on ice, to promote cell lysis. Next, the solution was centrifuged (7000 g, 10 min, 4°C) to discard cell debris. Sarcosine (Sigma, final concentration of 2%) was added to the supernatant and incubated for 20 min at 4 °C, to solubilize the OMPs. The solution was centrifuged (13000 g, 4 °C, 1 h), to recover the OMP that were ressuspended in Tris-HCl pH 7.4. The concentration of proteins was determined by Bicinchoninic Acid Protein Assay Kit and standardized to 240 ± 10 $\mu g.ml^{-1}$ in each sample and applied to a sodium dodecyl sulfate polyacrylamide gel electrophoresis with 12% bisacrylamide. The proteins were stained with Coomassie blue. Electrophoresis was accomplished at constant 170V.

Assessment of Quorum Sensing Inhibition: Quorum sensing inhibition was determined by the disc diffusion assay. The inoculum of *Chromobacterium violaceum* was grown overnight in Luria-Bertani broth (LB), (30 ± 3 °C, 150 rpm). The MIC and MBC for all chemicals were determined with the antibacterial susceptibility tests as described before, with minor modifications. LB broth was used and *C. violaceum* growth was determined at 620 nm. A standard disc diffusion assay was performed for all chemicals at the MBC. Briefly, the bacterial suspension (approximately 10^8 $CFU.ml^{-1}$), was seeded on LB agar plates using a sterilized swab. Next, sterile paper discs (6 mm diameter) were placed over the LB agar plates, and 15 µl of each biocide was added. Antimicrobial and quorum sensing inhibition (halo of colorless but viable cells) halos were measured after 24 h of incubation at 30 ± 3 °C.

RESULTS AND DISCUSSION:

1. Control of Biofilm: In order to determine the influence of a slowly-released antimicrobial on biofilm formation, *S. typhimurium* MAE52 cells were grown in the presence and absence of salicylic acid-based poly (anhydride ester) (SA-PAE) polymer fixed on glass coverslips The growth of *S. typhimurium* MAE52 and pH changes were elucidated in BHI broth at an initial pH of 7.2.

In the absence of SA-PAE, visible biofilms were formed at the liquid-air interface after 12 h of incubation, during the early stationary growth phase. The pH kinetics were recorded for 48 h of incubation and revealed their bimodal nature **Fig. 1A**.

During 12 h of incubation, the medium pH decreased significantly ($P<0.01$) from 7.2 to its lowest point of 5.6. Subsequently, the pH started to rise until it reached its highest point of 8.6 at 48 hours of incubation. There was no significant pH change for the remainder of the experiment **Fig. 1B**.

In the presence of the slowly-released SA, there was also a significant ($P<0.01$) decrease in pH to 5.2 after 12 h of incubation, and there was no significant change in the pH for the remaining time of the experiment **Fig. 1B**. Therefore, the bimodal nature of the pH was disrupted in the presence of released SA and there was no biofilm formation, despite the presence of a sufficient number of cells in the environment as compared to **Fig. 1A**.

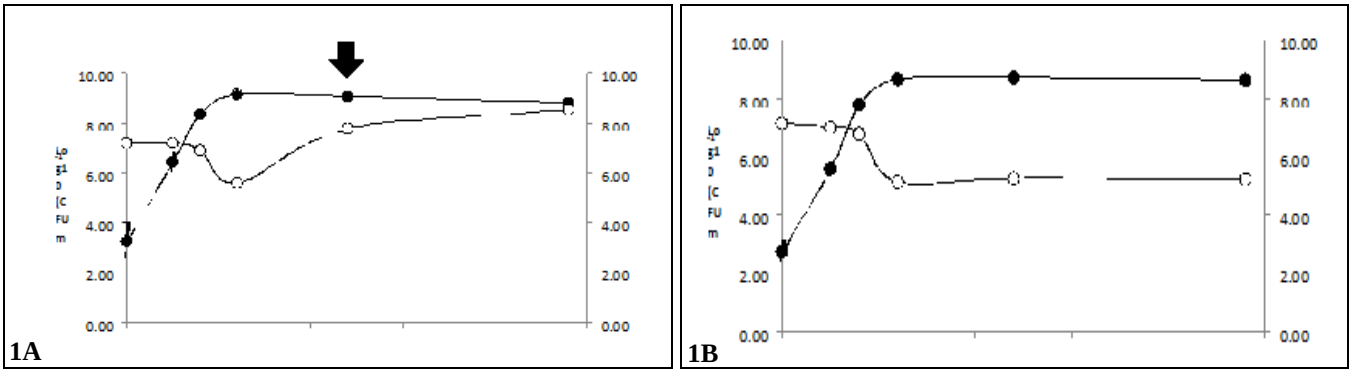

FIG. 1: CONTROLLED RELEASE OF SALICYLIC ACID DISRUPTS BIOFILM FORMATION AND BIMODAL pH KINETICS OF *S. TYPHIMURIUM* MAE52 GROWN AT INITIAL pH OF 7.2

2. Potent Antibacterial Nanoparticles against Biofilm Control: The water solubility of the nanoparticles suggests that the charged polar head group of phosphatidylcholine (PC) is accessible on the outer surface of PA NPs, which is beneficial for aminoglycoside binding. SEM images of the phosphatidylcholine decorated Au nanoparticles alone (PA NPs) or loaded with gentamicin (GPA NPs) showed that there was no visible morphological difference **Fig. 2A** and **B**. The average diameter of the GPA NPs was estimated to be ~180 nm by Image J software **Fig. 2C**. An explicit increase of about 65 nm in the hydrodynamic size of the Au NPs was detected after PC coating via dynamic light scattering (DLS) **Fig. 2D**, suggesting the formation of lipid bilayers.

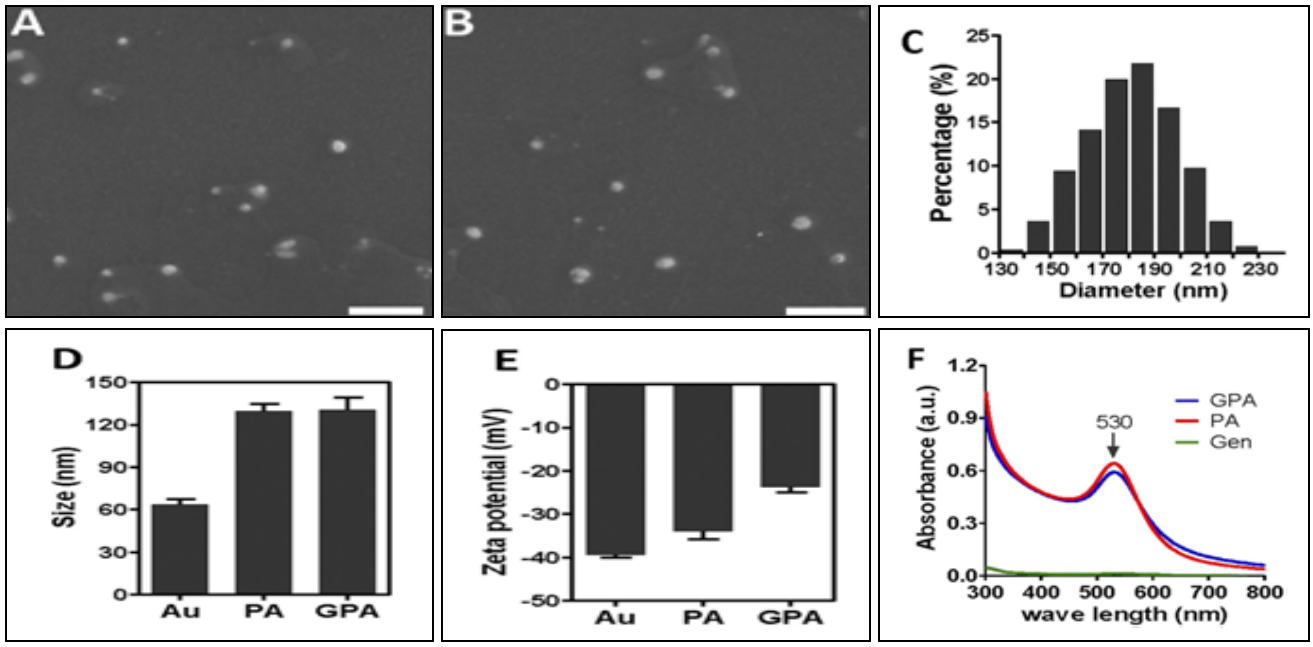

FIG. 2: SEM IMAGE OF PA NPs (A) AND GPA NPs (B); (C) SIZE DISTRIBUTION OF GPA ESTIMATED USING IMAGE J (ABOUT 1000 PARTICLES WERE COUNTED); (D) HYDRODYNAMIC SIZE AND (E) SURFACE ZETA POTENTIAL OF BARE AU NPS, PA NPs AND GPA NPs MEASURED BY DYNAMIC LIGHT SCATTERING; (F) ABSORPTION SPECTRUM OF PA NPs, GPA NPs AND GENTAMICIN. SCALE BAR REPRESENTED 1 MM

The binding of gentamicin seemed not to influence the size of nanoparticles further. The surface zeta potential changed from − 34.0 mV to − 24.7 mV **Fig. 3E**, which confirmed the binding of positively charged gentamicin to the charged polar head group of phosphatidylcholine on PANPs through electrostatic attraction. Both UV- visible spectra of PA NPs and GPA NPs revealed an identical absorbance peak at 530 nm, which suggested gentamicin load had no influence on the surface plasmon resonance of PA NPs **Fig. 2F**. The binding amount of gentamicin on the GPA NPs was estimated to be ~38 µg/mg (gentamicin/Au). The absorption of gentamicin on PA NPs reached the saturation point in 2 hours at both acidic and neutral pH **Fig. 3A**. It appeared that the acidic

condition facilitated the binding of the antibiotic. The increase of ionic strength led to a dramatic decrease in the loading of gentamicin on PA NPs **Fig. 3B**.

The release profile of gentamicin from GPA NPs indicated that GPA NPs were more stable at acidic pH **Fig. 3C** and lower ionic strength **Fig. 3D**.

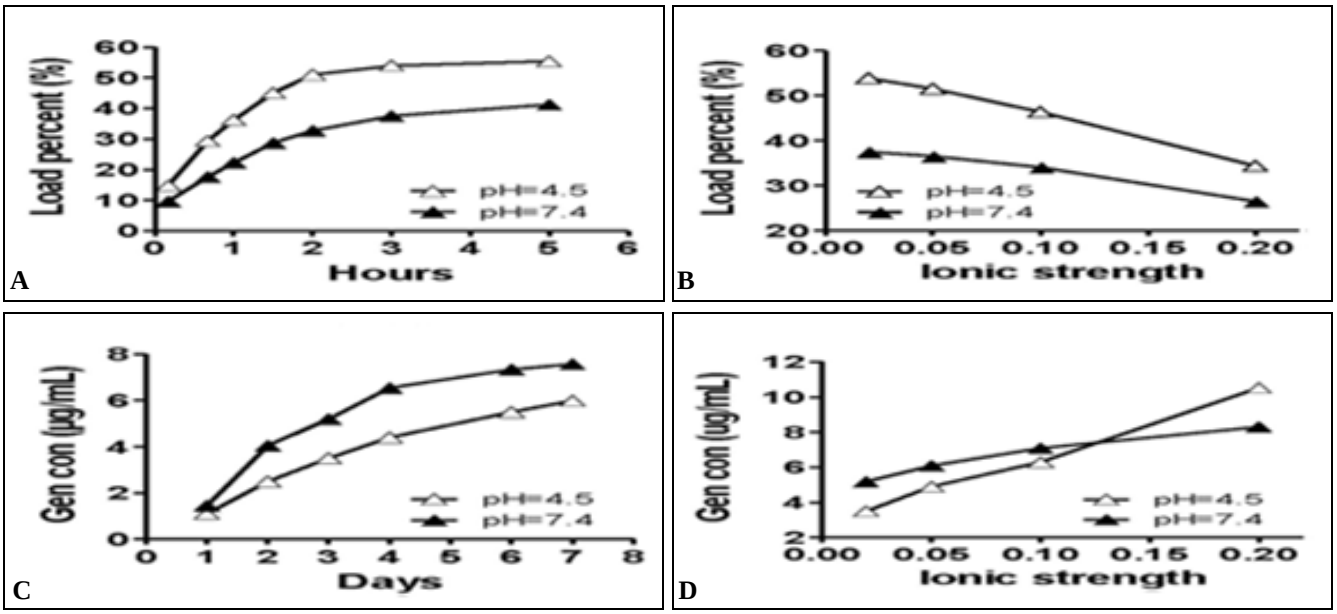

FIG. 3: THE LOAD (A) OR RELEASE PROFILES (C) OF GENTAMICIN ON GPA NPS IN 6 mm HEPES BUFFER (pH 7.4) AND 6 MMTRIS-HCL BUFFER (pH 4.5). THE EFFECT OF IONIC STRENGTH ON THE LOAD (B) OR RELEASE (D) OF GENTAMICINON GPA NPS. NaCl WAS ADDED TO 6 mm HEPES BUFFER (pH 7.4) AND 6 mm TRIS-HCL BUFFER (pH 4.5) TO OBTAIN THE IONIC STRENGTHS AS INDICATED

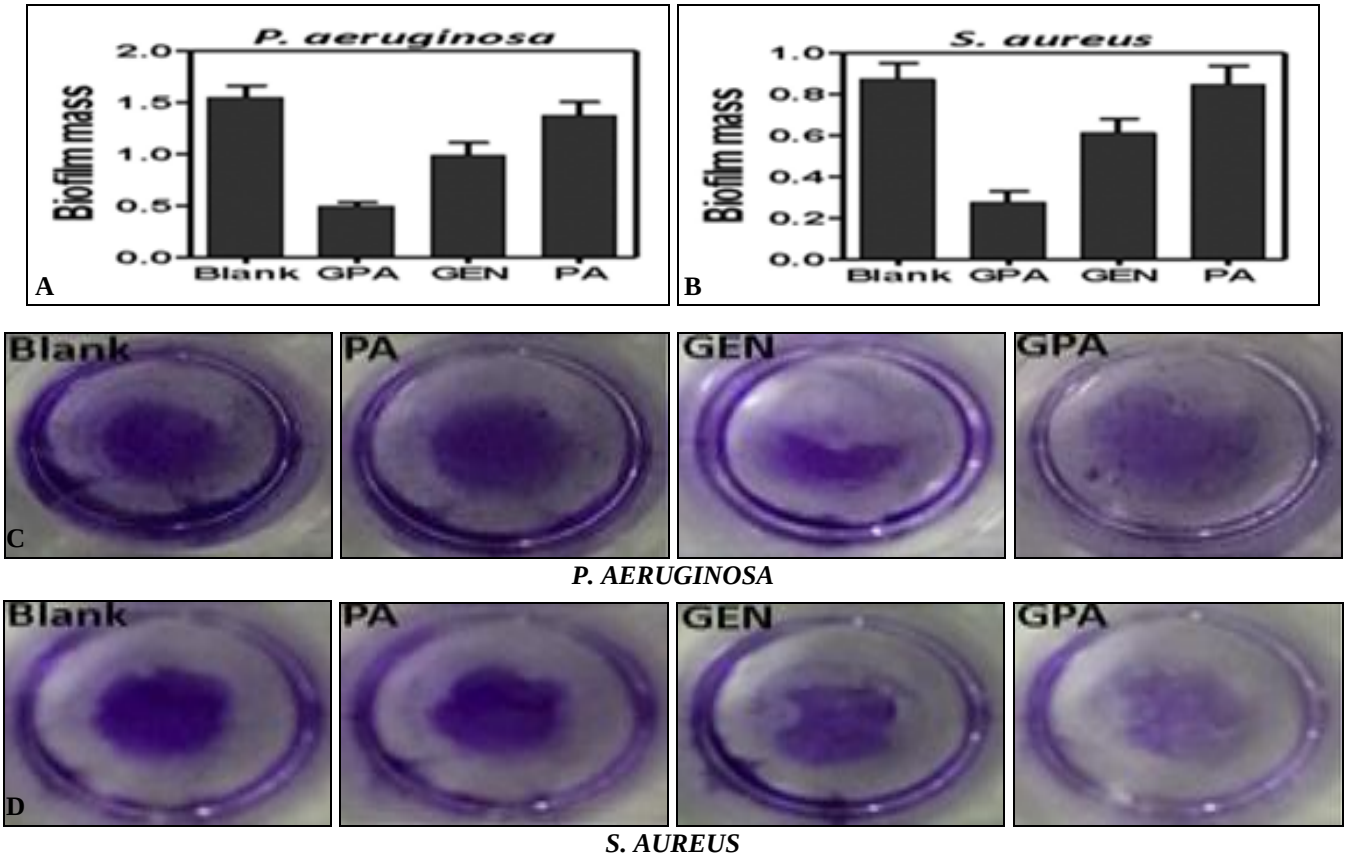

FIG. 4: CRYSTAL VIOLET ASSAY TO ASSESS THE ANTIBIOFILM ACTIVITY OF SAMPLES AGAINST *P. AERUGINOSA* BIOFILM (A, C) AND L. MONOCYTOGENES (B, D)

Antibiofilm Activities of GPA NPs: The antibiofilm efficacy of the particles was evaluated against both gram-positive and negative micro-organisms. A standard crystal violet assay for biofilm biomass indicated that GPA NPs were more effective in the eradication of preformed biofilm built by *P. aeruginosa* or *S. aureus* **Fig. 4**, than gentamicin or PA NPs alone did.

Similar findings were also observed in the case of biofilm built by *E. coli* **Fig. 4A,** and *L. monocytogenes* **Fig. 4.B**. Visualization of bacterial biofilms with scanning electron microscopy and fluorescence microscopy showed a wide spectrum of morphological differences in biofilm architectures **Fig. 5**. Besides, an equivalent amount of genta-micin (as in GPA NPs) was added to Au NPs, and no significant difference in the ability to disrupt biofilm was observed between gentamicin and gentamicin-carried gold nanoparticles (GA NPs) **Fig. 5**, which is in consistent with the earlier findings indicating no enhancement of the bactericidal activity of similar gentamicin-Au nanoparticles. Inhibition of biofilm formation was also examined in the case of planktonic *P. aeruginosa* **Fig. 6A** and *S. aureus* **Fig. 6B** exposed to reagents for 24 h at the beginning.

Quantification of biofilm biomass indicated that GPA NPs were superior to inhibit the biofilm formation of both bacteria above. Similar findings were also observed in the case of *E. coli* and *L. monocytogenes* **Fig. 7**.

Taken together, these results demonstrated that GPA NPs were more effective in inhibiting biofilm formation and disrupt preformed biofilms, regard-less of Gram-positive or Gram-negative organisms than gentamicin did.

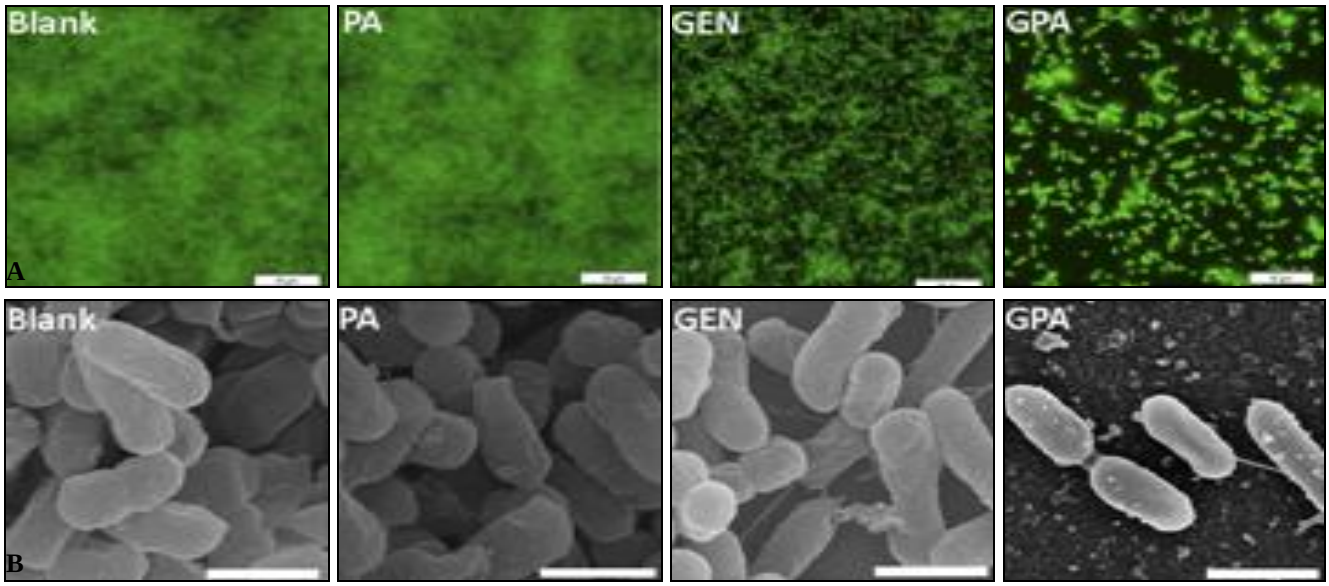

FIG. 5: FLUORESCENCE IMAGES (A) AND SEM IMAGES (B) OF P. AERUGINOSA BIOFILM. SCALE BAR FOR SEM AND FLUORESCENCE IMAGES ARE 1 µm AND 10 µm, RESPECTIVELY

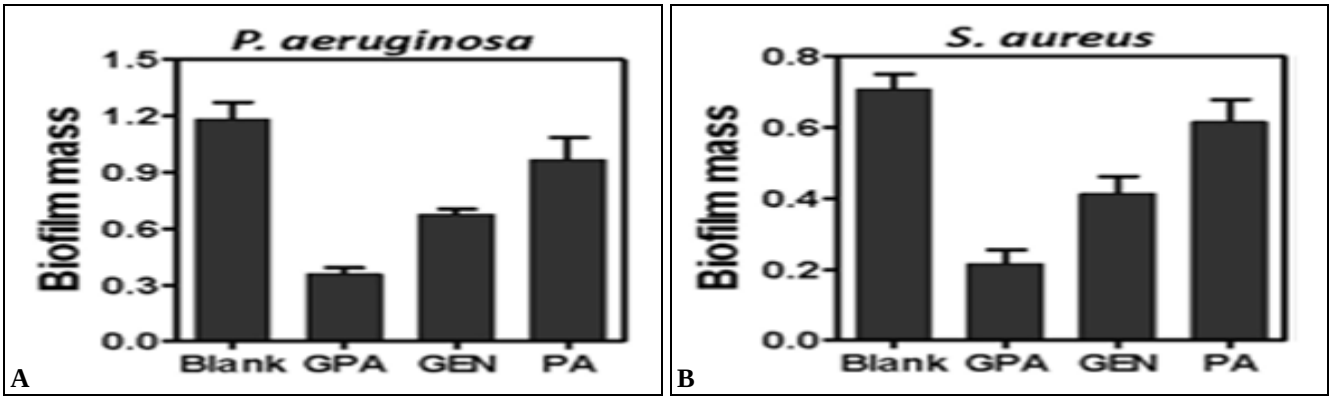

FIG. 6: THE INHIBITORY EFFECTS OF SAMPLES ON *P. AERUGINOSA* (A) AND *S. AUREUS* (B) BIOFILM FORMATION

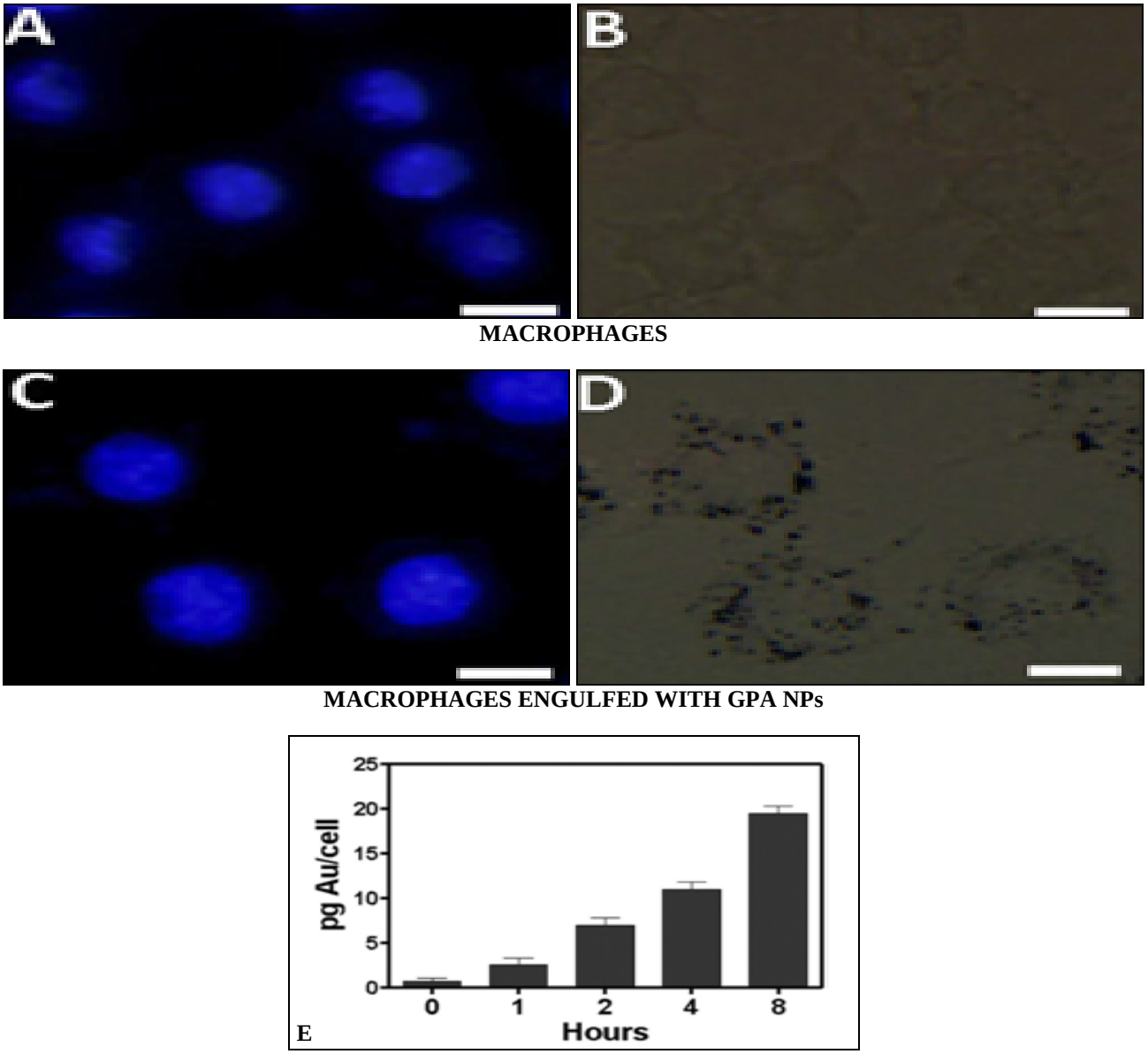

FIG. 7: FLUORESCENCE IMAGE (A, C) AND BRIGHTFIELD IMAGE (B, D) OF MACROPHAGES ALONE, OR MACROPHAGES INCUBATED WITH GPA NPS FOR 2 h FOLLOWED BY RINSING WITH NEW MEDIUM. SCALE BAR REPRESENTED 10 µm. (E) CELLULAR UPTAKE OF GPA NPs MEASURED BY ICP-MS. RAW264.7 CELLS WERE INCUBATED IN THE PRESENCE OF 0.116 mg/ml OF GPA NPs AS TIME INDICATED. DATA ARE REPRESENTED AS PG AU/CELL

TABLE 1: MINIMUM INHIBITORY CONCENTRATION (MIC) AND MINIMUM BACTERIAL CONCENTRATION (MBC) VALUES OF EACH CHEMICAL TESTED

	MIC/µg. mL^{-1}	MBC/µg. mL^{-1}
BrCl	650	700
BrOH	850	900
CTAB	20	50
SH	500	500

3. Nanoparticle-Based Compounds In Biofilm Control: The MIC and MBC values obtained for the tested chemicals against *P. fluorescence* are presented in **Table 1**. Overall, the MBC was higher than the MIC, with the exception of SH, in which a MIC and MBC were 500 µg.ml^{-1}. CTAB was the most efficient antimicrobial with an MBC 10 to 20 times lower than the other chemicals. *P. fluorescens* is naturally hydrophilic ($\Delta Gsws>0$ mJ.m^{-2}); however, this property was less pronounced when the cells were in contact with BrOH and CTAB ($P < 0.05$). The polar parameter (γsAB) of the bacterium increased with the application of CTAB and decreased in the presence of SH ($P < 0.05$). It was possible to observe that the treatment with SH significantly decreased the surface capacity of the cell to accept or donate electrons ($P < 0.05$), while BrOH and CTAB increased the electron acceptor component of *P. fluorescent* surface ($P < 0.05$). *P.*

fluorescens untreated cells had a negative surface charge of 13.53 mV with a conductivity of 0.05 $mS.cm^{-1}$ **Table 3**. The exposure to CTAB, BrCl or BrOH modified *P. fluorescens* surface charge to less negative and increased its conductivity ($P < 0.05$), with the exception of CTAB that had no effects on the cell surface conductivity ($P > 0.05$). **Table 4** shows the K^+ concentration with and without exposure to the chemicals. All chemicals tested promoted an alteration in the cytoplasmic membrane permeability, causing K^+ release, regardless of the chemical used ($P < 0.05$).

TABLE 2: SURFACE TENSION PARAMETERS, HYDROPHOBICITY (Δ), APOLAR (*γsLW*) AND POLAR (*γsAB*), OF UNTREATED *P. FLUORESCENS* (CONTROL) AND AFTER 1 h TREATMENT WITH THE CHEMICALS (BRCL, BROH, CTAB OR SH).

Surface tension parameters/mJ.M-2 / ΔGsws/mJ.m^{-2}						
	γ_s^{LW}	γ_s^{AB}	γ_s^{+}	γ_s^{-}		
Control	22.8± 4.43	30.3± 4.79	4.14±1.25	57.0 ±4.71	30.7± 6.30	Control
BrCl	19.4± 0.43	31.4± 2.92	4.40±1.07	57.0 ±3.96	29.8 ± 5.50	BrCl
BrOH	20.3± 0.80	34.1± 3.61	6.10±1.25	53.0 ±3.51	23.4 ± 4.90	BrOH
CTAB	12.0± 1.35	47.0± 7.10	10.4±2.9	54.0 ±0.8	14.0 ± 5.00	CTAB
SH	29.4± 4.68	13.3± 1.83	0.89±0.33	51.0 ±6.00	33.5 ± 8.70	SH

The average ± SD is presented

TABLE 3: ZETA POTENTIAL AND CONDUCTIVITY OF *P. FLUORESCENCE* BEFORE AND AFTER 1 h TREATMENT WITH DIFFERENT CHEMICALS

	Zeta potential/Mv	Conductivity /mS. Cm^{-1}
Control	-13.5 ± 2.32	0.05 ± 0.02
BrCl	-2.88 ± 0.66	2.25 ± 0.06
BrOH	-4.96 ± 0.95	0.46 ± 0.09
CTAB	-8.14 ± 0.42	0.05 ± 0.01
SH	-13.0 ± 1.41	31.1 ± 0.14

The average ± SD is presented

TABLE 4: CONCENTRATION OF K+ IN SOLUTION OF THE UNTREATED AND AFTER 1 h INCUBATION OF *P. FLUORESCENCE* WITH EACH CHEMICAL

Concentration of k^+ in solution / µg.mL^{-1}	
Control	1.21 ± 0.08
BrCl	1.99 ± 0.21
BrOH	1.96 ± 0.25
CTAB	2.09 ± 0.28
SH	2.07 ± 0.26

The average ± SD is presented

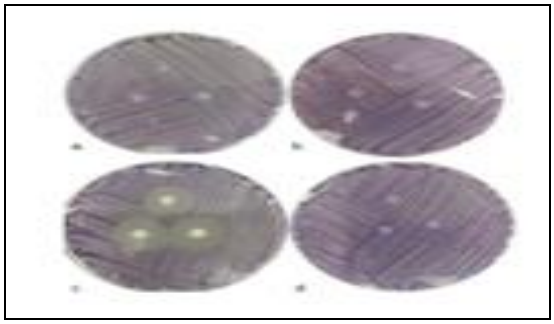

FIG. 8: DISC DIFFUSION ASSAYS FOR THE DETECTION OF QUORUM SENSING INHIBITION OF *C. VIOLACEUM* BY (A) BROH, (B) BRCL, (C) SH AND (D) CTAB.

The OMP expression, using 1-D SDS-PAGE, was assessed before and after biocide exposure for 1 h **Fig. 8**. No significant differences were found in the expression of the major OMP of *P. fluorescens* with and without the exposure to the selected chemicals, with the exception that CTAB and SH reduced significantly the amount of OMP expressed in **Fig. 9**.

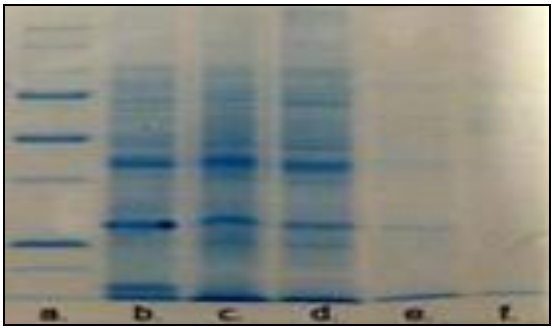

FIG. 9: OMP PROFILE OF P. FLUORESCENS CELLS WHEN EXPOSED TO THE MBC OF DIFFERENT CHEMICALS. THE MOLECULAR WEIGHT MARKER (A) WAS USED TO EXTRAPOLATE THE MOLECULAR WEIGHT OF SOME LANES OF THE OMP PROFILE OBTAINED FROM INCUBATION IN THE (B) ABSENCE OR IN THE PRESENCE OF (C) BRCL, (D) BROH, (E) CTAB AND (F) SH

Table 5 shows retardation caused by *P. fluorescens* biofilms for each chemical used. Data are presented as average ± SD of the percentage of diameter measurements for halo readings compared with controls (no biofilm).

TABLE 5: RETARDATION CAUSED BY *P. FLUORESCENS* BIOFILMS, FOR EACH CHEMICAL, USED

Retardation/ %	
BrCl	BrCl
BrOH	BrOH
CTAB	CTAB
SH	SH

The effectiveness of the chemicals was assessed in terms of number of biofilm CFU **Fig. 10A** and mass **Fig. 10B**. The results obtained for the number of biofilm CFU revealed a reduction after 1 h exposure to the MBC of CTAB and SH **Fig. 3A**. However, this effect was more pronounced for SH with 1-log reduction ($P > 0.05$).

In order to ascertain the role of the chemicals tested on biofilm regrowth, the CFU was determined during the 2, 12, and 24 h after chemical exposure. Two hours after the treatment, the number of CFU increased for all chemicals tested, attaining similar values to those before the treatment. The number of biofilm CFU, remained constant overtime for all the conditions tested, except for the 24 h BrCl-treated biofilms. In this case, the number of CFU increased significantly ($P < 0.05$, **Fig. 10A**) when compared to the control values (untreated biofilms).

In terms of biofilm mass, the three chemicals promoted similar biomass removal (16%, **Fig. 11B**). Remained unchanged 2 h after the treatment ($P > 0.05$). When analyzing the biofilm, 12 h after the treatment, no significant biomass changes were found for the biofilms treated with CTAB and BrCl, in comparison to the biofilms immediately after exposure.

The SH treated biofilms recovered significantly in terms of biomass ($P < 0.05$). However, 24 h after the treatment, the values obtained for the biomass were as low as the values achieved with the SH treatment after the same time. During the recovery period, the biomass of CTAB-treated biofilms was similar to the value immediately after the treatment, while significant biomass regrowth of the BrCl-treated biofilms was found ($P > 0.05$).

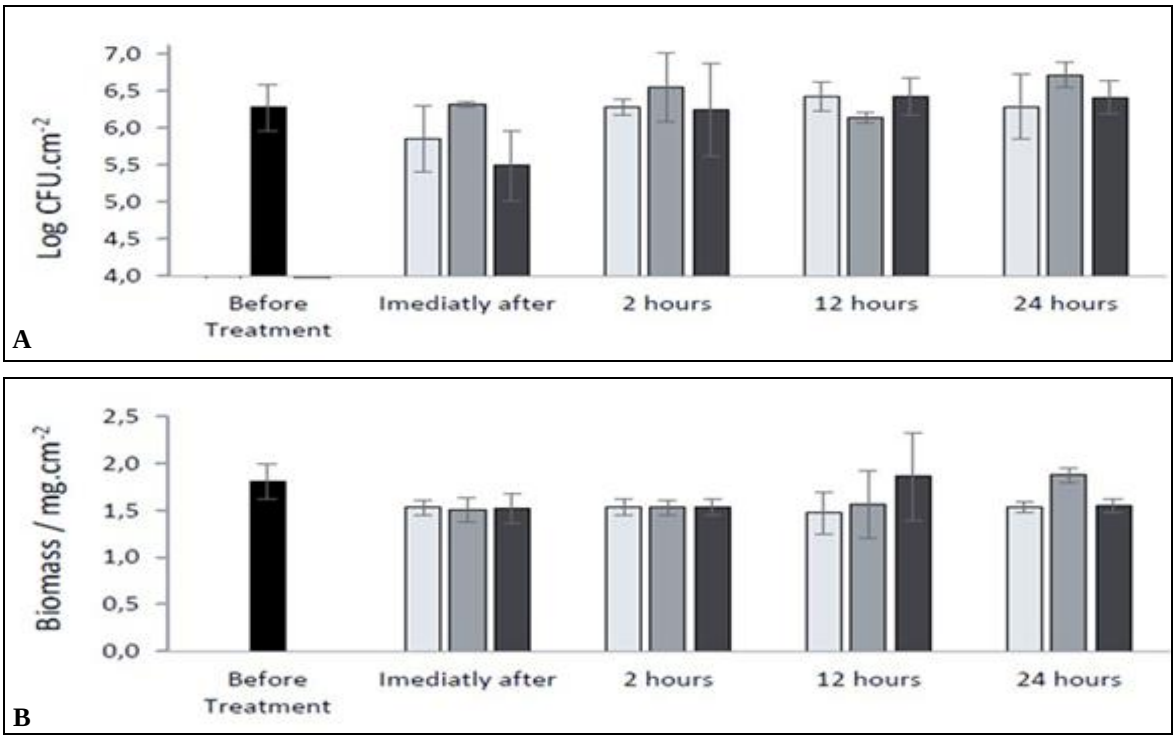

FIG. 10: FLUORESCENS BIOFILM LOG CFU. CM-2 (a) AND MASS (b) BEFORE AND AFTER TREATMENT WITH CTAB ( ) BRCL ( ) AND SH ( ). SAMPLE WERE COLLECTED BEFORE TREATMENT ( ), IMMEDIATELY AFTER 1HRS TREATMENT AND AFTER 2, 12 AND 24 H AFTER CHEMICAL REMOVAL. Values are average ± SD.

CONCLUSION: Despite the advances mode in the development of novel Antibiofilm agents, devised biofilm treatment strategies are limited by their high costs and complexities, which means urgent development is required to identify cost-efficient alternatives. As is made clear by this thesis, recent developments in nanotechnology-based approaches aimed at preventing, controlling, and treating bacterial biofilm infections, especially biomedical devices, are worthy of serious consideration.

ACKNOWLEDGEMENT: Nil

CONFLICTS OF INTEREST: Nil

REFERENCES:

1. Whitchurch CB, Tolker-Nielsen T, Ragas PC and Mattick JS: Extracellular DNA required for bacterial biofilm formation. Science 2002; 295(5559): 1487.
2. Lewis K: Persister cells and the riddle of biofilm survival. Biochemistry 2005; 70(2): 267-74.
3. Mah TFC and O'Toole GA: Mechanisms of biofilm resistance to antimicrobial agents. Trends in Microbiology 2001; 9(1): 34-39.
4. Dongari-Bagtzoglou A: Pathogenesis of mucosal biofilm infections: challenges and progress. Expert Review of Anti-Infective Therapy 2008; 6(2): 201-08.
5. Nikolaev YA and Plakunov VK: Biofilm city of microbes or an analogue of multicellular organisms? Microbiology 2007; 76(2): 125-38.
6. Allegranzi B, Nejad SB and Combescure C: Burden of endemic health-care-associated infection in developing countries: systematic review and meta-analysis. The Lancet 2011; 377(9761): 228-41.
7. Zarb P, Coignard B and Griskeviciene J: The European Centre for Disease Prevention and Control (ECDC) pilot point prevalence survey of healthcare-associated infections and antimicrobial use. Euro Surveillance 2012; 17(46, article 2).
8. Torrecillas R, Díaz M, Barba F, Miranda M, Guitian F and Moya JS: Synthesis and antimicrobial activity of a silver-hydroxyapatite nanocomposite. Journal of Nanomaterials 2009; 2009: 6.
9. Stanixc V, Janackovic D and Dimitrijevic S: Synthesis of antimicrobial monophase silver-doped hydroxyapatite nanopowders for bone tissue engineering. Applied Surface Science 2011; 257(9): 4510-18.
10. Pattani VP and Tunnell JW: Nanoparticle-mediated photothermal therapy: a comparative study of heating for different particle types. Lasers in Surgery and Medicine 2012; 44(8): 675-84.
11. Taylor E and Webster TJ: Reducing infections through nanotechnology and nanoparticles. International Journal of Nanomedicine 2011; 6: 1463-73.
12. Prudencio A, Schmeltzer RC and Uhrich KE: Effect of Linker Structure on Salicylic Acid Derived Poly (anhydride−esters). Macromolecules 2005; 38: 6895-01.
13. Busscher HJ, Weerkamp AH, Vander mei HC, VanPelt AWJ, DE Jong HP and Arends J: Measurement of the surface free energy of bacterial cell surfaces and its relevance for adhesion 1984; 48(5): 980-83.
14. Ferreira C, Pereira A, Pereira M, Melo L and Simoes M: Physiological changes induced by the quaternary ammonium compound benzyldimethyldodecylammonium chloride on Pseudomonas fluorescens. Journal of Antimicrobial Chemotherapy 2011; 66(5): 10361043
15. Winder CL, Al-Adham ISI, Malek SMAA, Buultjens TEJ, Horrocks AJ and Collier PJ: Outer membrane protein shifts in biocide-resistant *Pseudomonas aeruginosa* PAO1. Journal of Applied Microbiology 2000; 89(2): 289-95.

How to cite this article:
Patel C and Tripathi N: The potential role of nanotechnology to control of industrial biofilm. Int J Pharm Sci & Res 2020; 11(11): 5831-43. doi: 10.13040/IJPSR.0975-8232.11(11).5831-43.